



Published in final edited form as:

*J Interferon Cytokine Res.* 2007 May ; 27(5): 383–392. doi:10.1089/jir.2006.0067.

## The IFN- $\beta$ and Retinoic Acid-Induced Cell Death Regulator GRIM-19 Is Upregulated During Focal Cerebral Ischemia

ZARA MEHRABIAN<sup>1</sup>, KRISH CHANDRASEKARAN<sup>1</sup>, SUDHAKAR KALAKONDA<sup>2</sup>, TIBOR KRISTIAN<sup>1</sup>, GARY FISKUM<sup>1</sup>, and DHANANJAYA V. KALVAKOLANU<sup>2</sup>

<sup>1</sup> Department of Anesthesiology, University of Maryland School of Medicine, Baltimore, MD 21201

<sup>2</sup> Department of Microbiology and Immunology, University of Maryland School of Medicine, Baltimore, MD 21201

### Abstract

The induction of GRIM-19 has been shown to be essential for interferon- $\beta$  (IFN- $\beta$ )-induced and retinoic acid (RA)-induced tumor cell death. We have studied the localization and levels of GRIM-19 in IFN/RA-induced cell death in neural cells and in focal cerebral ischemia. Exposure to IFN/RA caused a ~15-fold increase in GRIM-19 protein levels and induced >50% cell death in human neuroblastoma SH-SY5Y cells. In rats subjected to permanent focal cerebral ischemia, increased oxidative stress, as well as increased GRIM mRNA levels (32-fold) and increased GRIM-19 (>50%) protein levels were noted in the ipsilateral (affected) hemisphere compared with the contralateral (unaffected) hemisphere. These results suggest that GRIM-19 may play a role in ischemia-induced neuronal cell death.

### INTRODUCTION

Mitochondria are a subcellular target of ischemic brain injury.<sup>1</sup> Decreased ATP production, increased re-active oxygen species (ROS) generation, and the release of proapoptotic mitochondrial proteins have been implicated as possible mechanisms by which injury causes cell death.<sup>2–4</sup> The extent to which individual components of the mitochondrial respiratory chain complex participate in each of these mechanisms is an area of interest.

Cytokines, such as interferons (IFNs), suppress cell growth and participate in stress-induced physiologic responses. Previously, it was shown that a combination of IFN- $\beta$  and retinoic acid (RA) causes increased cell death of some solid tumor cells that are not significantly affected by IFN alone.<sup>5,6</sup> GRIM-19 has been identified as one of the genes associated with RA/IFN- $\beta$ -induced mortality in breast carcinoma cells.<sup>7</sup> Downregulation of GRIM-19 expression via antisense-mediated approaches promotes cell growth in the presence of IFN/RA-induced cell death.<sup>8</sup> The apoptotic effect of GRIM-19 protein is ablated by viral oncogenic proteins.<sup>9</sup> More recently, tumor-specific mutations in GRIM-19 have been identified.<sup>10,11</sup>

GRIM-19 has also been identified to be a previously unknown 17-kDa subunit protein of complex I of the mitochondrial respiratory chain.<sup>12</sup> Complex I consist of 46 proteins,<sup>11</sup> catalyzes the first step of the electron transfer, and is one of the major sites of ROS production

Address reprint requests or correspondence to: Dr. Zara Mehrabian, Department of Anesthesiology, University of Maryland School of Medicine, MSTF 5–34; 685 W Baltimore Street, Baltimore, MD 21201, Tel: (410) 706-2388, Fax: (410) 706-2550, E-mail: zmehr001@umaryland.edu, Dr. Dhan V. Kalvakolanu, Department of Microbiology and Immunology, University of Maryland School of Medicine, 660 W Redwood Street, Baltimore, MD 21201, Tel: (410) 328-1396, Fax: (410) 328-6559, E-mail: dkalvako@umaryland.edu.

in mitochondria.<sup>14</sup> Deletion of GRIM-19 destroys the assembly and electron transfer activity of complex I and influences other complexes in the mitochondrial respiratory chain.<sup>13</sup> These observations demonstrate that GRIM-19, a gene product with a specific role in IFN/RA-induced cell death, is also a functional component of the mitochondrial oxidative phosphorylation system (OXPHOS).<sup>14</sup>

Although the growth-suppressive effects of GRIM-19 in cancer cells are relatively clear, its role in other pathologic responses remains largely unknown. Our interest in GRIM-19 in cerebral ischemia arose from the observations of Schneider et al.<sup>15</sup> that transcriptional alterations in GRIM-19 occur during permanent focal ischemia. In this study, we investigated the localization and expression of GRIM-19 in neuronal cultures. We compared the levels of GRIM-19 protein and mRNA in the affected and unaffected brain regions after cerebral ischemia. Our results show a significant upregulation of GRIM-19 in synaptosomes of the affected regions of the brain. This increase in GRIM-19 protein levels is correlated with increased oxidative stress. These results suggest a role for GRIM-19 in ischemia-induced cell death.

## MATERIALS AND METHODS

### Chemicals

Universal type I IFN was purchased from PBL Biomedical Labs (Piscataway, NJ). Anti-GRIM-19 antibody was purchased from Mitosciences (Eugene, OR). Antiporin antibody was purchased from Calbiochem (La Jolla, CA). All other reagents were purchased from Sigma (St Louis, MO), unless stated otherwise.

### Cell culture

Human neuroblastoma SH-SY5Y cells were maintained in Dulbecco's modified essential medium (DMEM), with 10% fetal bovine serum (FBS) and 1% penicillin/streptomycin. Primary cultures of cortical neurons were prepared from the cerebral hemispheres of 16-day gestation rat embryos using a modification of the methods of Yavin and Yavin.<sup>16</sup> Astrocytes were prepared from rat brain (1-day-old pups) using a method based on a procedure by Booher and Sensenbrenner.<sup>17</sup>

### Treatment with IFN- $\beta$ and RA

Human neuroblastoma SH-SY5Y cells were exposed in the culture medium to either vehicle (ethanol; final concentration <0.01%) or *all-trans* RA (final concentration 1  $\mu$ M) or IFN- $\beta$  (final concentration 500 U/mL) or a combination of RA and IFN- $\beta$  for 48 h. Cell death was measured by staining with propidium iodide (PI) (nonviable cells, red fluorescence) and SYTO-13 (viable cells, green fluorescence) and quantified as a percentage of dead over total number of cells. Nine replicates for each treatment group (three separate experiments with three fields in each well) were used, and the data were expressed as the mean  $\pm$  SEM.

### Transfection

To determine the localization of GRIM-19 to mitochondria, SH-SY5Y human neuroblastoma cells were transfected with pmito-eYFP vector (Clontech Laboratories, Mountain View, CA). Transfection with the plasmid was done with Lipofectamine 2000 following the manufacturer's protocol (Invitrogen, Carlsbad, CA). Cells expressing mitochondrial eYFP were visualized 16 h after transfection and were used. Approximately 30% of the cells were found to express eYFP within mitochondria under these conditions.

## Immunolocalization

Cells expressing eYFP were fixed with 4% paraformaldehyde, permeabilized with 0.1% Triton X-100, blocked with 5% normal goat serum  $\pm$  1% bovine serum albumin (BSA), immunolabeled with 0.125  $\mu$ g/mL GRIM-19 antibody overnight at 4°C, rinsed, and incubated with goat antimouse IgG conjugated with Alexa Fluor 546 fluorescent label (1:500) (Molecular Probes, Invitrogen, Carlsbad, CA).

## Focal ischemia

All animal experiments were done in compliance with the National Institutes of Health (NIH) guidelines and approved by the University of Maryland Animal Care and Use Committee. Briefly, overnight fasted male Wistar rats, weighting 270–330 g, were anesthetized with 3.5% halothane in a mixture of N<sub>2</sub>O:O<sub>2</sub> (70:30). The animals were allowed to breathe spontaneously with inhalation of 1.5% halothane. A polyethylene catheter was inserted into a tail artery for blood pressure recording and blood sampling. A thermistor probe was placed in the rectum. With the help of an external heating lamp, the core temperature was maintained at 37°  $\pm$  0.5° C during the operation. A skin incision was made in the middle of the neck, and the right internal carotid artery was exposed from the carotid bifurcation to the basal cranium at the site of tympanic bulla. The external carotid and the occipital arteries were ligated. The common carotid artery was closed by ligature. A small incision was made in the common carotid artery, and the occluder (monofilament fishing line, 0.25 mm in diameter with a distal cylinder of silicon rubber) was inserted into the internal carotid artery through the common carotid artery. The occluder was then further advanced to the origin of the middle cerebral artery (MCA) and fixed by the surgical suture. Heparin (0.2 mL, 250 U/mL) was administered just before induction of ischemia. After these surgical procedures, anesthesia was discontinued, and animals were allowed to wake up. Twenty-four hours after the induction of ischemia, the brains were quickly removed, and ipsilateral and contralateral hemispheres were separated and used for mitochondria, RNA, and protein isolation.

To document the infarct area after focal ischemia 2,3,5-tri-phenyltetrazolium hydrochloride (TTC) staining was used.<sup>18</sup> Briefly, brains were rapidly removed and sectioned at 2-mm intervals. Sections were immersed in 2% TTC in buffered Ringer's solution at pH 7.4 (37.5° C) for 20 min and then transferred to 4% formaldehyde buffer for 15 min before photography.

## Isolation of mitochondria from brain

Synaptosomes and nonsynaptic mitochondria from contralateral and ipsilateral hemispheres of rat brain subjected to the focal ischemia were isolated according to Kristian et al.<sup>19</sup> Briefly, after decapitation, the forebrain was rapidly removed and placed in ice-cold mannitol-sucrose (MS) buffer, pH 7.4 (225 mM mannitol, 75 mM sucrose, 5 mM HEPES, 1 mg/mL fatty acid-free BSA, 1 mM EGTA). The brain was homogenized, then centrifuged twice at 1300g for 3 min. The collected supernatant was centrifuged for 10 min at 21,074g, and the pellet was resuspended in 15% Percoll (Amersham Biosciences, Piscataway, NJ), then layered on a discontinuous Percoll gradient (23% Percoll layered over 40% Percoll) and spun at 29,700g for 8 min. Discontinuous Percoll gradient allows a separation of mitochondria from cell debris in the homogenates on the basis of density. The nonsynaptosomal mitochondrial fraction located at the 40% and 23% Percoll interface was centrifuged at 16,600g for 10 min. Synaptosomes were located at the 15% and 23% Percoll interface. The nonsynaptic mitochondrial pellet was resuspended in the isolation buffer, but without BSA or EGTA, and spun at 7000g for 10 min. The synaptosomal layer was collected, resuspended in the isolation buffer, but without BSA or EGTA, and spun at 16 600g for 10 min. Pellets were collected separately and were used as synaptosomes and nonsynaptosomal mitochondria. Protein concentrations were determined by the method described by Lowry et al.<sup>20</sup>

### Isolation of mitochondria from cultured cells

Mitochondria from cultured primary cells (cortical astrocytes and neurons) were isolated by a nitrogen cavitation technique described by Kristian et al.<sup>21</sup> The cells ( $2 \times 10^8$ ) were washed with isolation medium (225 mM mannitol, 75 mM sucrose, 5 mM HEPES, 1 mM EGTA, pH 7.4 at 4°C), then scraped in 3 mL of the isolation medium and collected into a cavitation chamber (nitrogen bomb) (Parr Instrument Company, Moline, IL). The cell suspension under stirring was subjected to 1500 psi for 15 min. At the end of the 15 min period, the pressure in the chamber fell to approximately 800 psi. The cell suspension was then released through outflow tubing attached to the valve localized at the bottom of the cavitation chamber. Thus, the depressurization of the cell suspension from 800 psi to normal atmospheric pressure was instantaneous. After collection of the cell suspension from the cavitation chamber, it was centrifuged at 1500g for 3 min to pellet the cell debris (heavy particles, or fractions of cells). The supernatant was collected and centrifuged at 20,000g for 10 min. The pellet (crude mitochondrial fraction) was resuspended in 0.8 mL of 15% Percoll and layered on a preformed gradient consisting of 21% (for neuronal mitochondria) or 23% (for astrocytic mitochondria) Percoll (2 mL) layered over 50% Percoll (0.8 ml) in a 4-mL centrifuge tube. Following centrifugation of the gradient at 30,700g for 6 min, the mitochondria accumulated at the lower interface (between the 50% and 21% Percoll layers). The top layers were removed, and the mitochondrial fractions were collected and diluted with isolation medium (1:8). After centrifugation at 17,000g for 10 min, the pellet (purified mitochondria) was diluted with 1.5 mL of isolation medium and centrifuged at 7000g for 10 min. The final pellet was resuspended in 30  $\mu$ L of isolation medium without EGTA.

### Isolation of total RNA and RT-PCR

Total RNA was isolated from contralateral and ipsilateral brain hemispheres after 24 h of permanent cerebral ischemia, using RNA-Bee-RNA isolation solvent (Tel-Test, Inc, Friendswood, TX) following the manufacturer's protocol. To access levels of transcripts of GRIM-19 in brain tissue, primers specific for GRIM-19 (forward, ACCGGAAGTGTGGGATACTG; reverse, GCTCACGGTTCCTTTCATT) were used, and  $\beta$ -actin was used to normalize the cDNA input levels.

The iScript One-step RT-PCR kit with cyber green (Bio-Rad, Hercules, CA) was used for real-time quantitative PCR of RNA templates. RQ-PCR was performed on the Bio-Rad I-cycler optical module. Reactions were performed in a 50- $\mu$ L volume containing RNA, 0.5  $\mu$ M each of forward and reverse primers, and buffer included in the master mix (SYBR green I, Qiagen, Chatsworth, CA). PCR cycling conditions were reverse transcription step for 10 min at 50°C, followed by an initial denaturation step at 95°C for 3 min, then 50 cycles of 1 min of denaturation at 95°C and 1 min of annealing and extension at 59.5°C, and final extension. Cycle threshold (Ct) values for  $\beta$ -actin and GRIM-19 were obtained.  $\Delta$ Ct were calculated by subtracting the  $\beta$ -actin Ct value from the GRIM-19 Ct value.  $\delta\Delta$ Ct were calculated by subtracting the contralateral  $\Delta$ Ct value from the ipsilateral  $\Delta$ Ct value. The fold change was determined using the formula  $2^{-\delta\Delta\text{Ct}}$ .

### Apoptosis

Cell death was measured using FACS after treating cells with various agents as described previously,<sup>22</sup> and the sub-G1 peak was counted and plotted. In addition, cell death was measured by direct counting of cells using the trypan blue exclusion method.

### Western blot analysis

Isolated mitochondria were treated with 50 mM dithiothreitol (DTT) and NuPage 4  $\times$  LDS loading buffer (Invitrogen) and heated at 70°C for 15 min. The samples were rapidly

centrifuged at 4°C and separated on SDS-PAGE. Each lane was loaded with 10  $\mu$ g mitochondrial protein, which was determined in separate studies to be in the linear range of the protein-immunoblot optical density (OD) relationship. Immunoblotting was performed as recommended by the manufacturers of the antibodies. The proteins were transferred to PVDF membrane, and the blot was divided horizontally according to appropriate molecular weight. The blots were incubated with different antibodies. Both the top and bottom portions of the blot were processed at the same time. Immunoreactivity was detected using the appropriate peroxidase-linked secondary antibody and enhanced chemiluminescence (ECL) detection reagent purchased from Amersham Biosciences (GE Healthcare, Piscataway, NJ). ODs of individual bands on the Western blots were quantified after subtraction of background levels (taken from adjacent areas of the same film) using the GelExpert software program (Nucleotech, San Carlos, CA).

### Oxyblot

Oxidative modification of proteins that increase carbonyl groups was assessed by Oxyblot (Chemicon, Temecula, CA).

## RESULTS AND DISCUSSION

### Exposure of neuronal cells to IFN and RA increases levels of GRIM-19 and induces cell death

The combination of RA and IFN- $\beta$  has been shown to induce cell death in breast cancer cell lines.<sup>7</sup> To determine if IFN/RA exerts similar growth-suppressive effects in the cells derived from the central nervous system, human neuroblastoma SH-SY5Y cells grown in culture dishes were treated either with vehicle, IFN, RA, or a combination of IFN/RA. The results are shown in Figure 1A. Exposure of SH-SY5Y cells to RA alone induced a morphologic differentiation but did not cause cell death (Fig. 1A). Similarly, exposure to IFN alone did not cause significant cell death (Fig. 1A), whereas combined exposure to IFN/RA for 48 h caused an increase in cell death (Fig. 1A). Indeed, this rise in cell death correlated with a corresponding rise in the level of GRIM-19 in IFN/RA-treated cells. IFN and RA alone did not cause a significant increase in the GRIM-19 protein levels. Quantification of cell death in SYTO-13 cells (viable cells, green fluorescence) showed a ~7-fold increase in cell death in IFN/RA-treated neural cells ( $60 \pm 4$  SYTO-13-positive/field in vehicle-treated vs.  $8 \pm 1$  SYTO-13-positive/field in IFN/RA-treated cells). Cell death was also measured using flow cytometry. Cells were exposed to various agents and stained with PI. The percentage of cells in the sub-G1 peak was measured in each case, and the data were plotted (Fig. 1B). Whereas there was a baseline amount of death (~10%) in cells treated with the individual drugs, IFN/RA treatment caused a significant rise in apoptotic cells (~73%). Plating SH-SY5Y neuroblastoma cells at a low density and then exposing them to IFN, RA, or IFN/RA showed that IFN/RA exhibits a dual effect on cell growth: (1) inhibition of cell growth and (2) an induction of cell death (as evidenced by SYTO-13 and PI staining) (Fig. 1E,F,G). Thus, our results extend the results obtained in breast carcinoma cell lines to neuronal cells to suggest that IFN/RA treatment-induced cell death. In breast cancer cell lines, death by the IFN/RA combination has been shown to be apoptotic.<sup>7</sup>

To determine if the cell death could be correlated with the expression of GRIM-19, cells were exposed to IFN/RA for various lengths of time, and equal quantities of protein lysates from each treatment were used for Western blot analysis with GRIM-19 (Fig. 1C). A time-dependent increase in GRIM-19 levels was observed. Exposure to IFN/RA for 48 h increased the GRIM-19 protein levels by ~15-fold compared with control. A comparable loading and transfer of proteins in the blot was ascertained by probing the same blot with  $\beta$ -actin-specific antibodies. Exposure of cells to IFN or RA alone did not change the levels of GRIM-19 (Fig. 1D) compared with the vehicle control. These results show that even after correcting for cell death, exposure

to IFN/RA increases the levels of GRIM-19 protein in the human neuroblastoma cell line SH-SY5Y.

### Localization of GRIM-19 to mitochondria

Previous studies showed that GRIM-19 interacts with signal transducer and activator of transcription 3 (Stat3)<sup>8</sup> and is also a component of the mitochondrial electron transport chain, one of the subunits of complex I (NADH dehydrogenase). We examined the localization of GRIM-19 with anti-GRIM-19 antibody in SH-SY5Y cells that were transfected with a vector that encodes mitochondrially targeted eYFP protein. The results are shown in Figure 2A,B,C. The majority of GRIM-19 staining coincided with eYFP fluorescence, suggesting that GRIM-19 is predominantly localized to mitochondria in these cells. In IFN/RA-treated eYFP-transfected SH-SY5Y cells, the merged image showed a decrease in intensity in colocalization, suggesting the possible presence of GRIM-19 in mitochondrial and nonmitochondrial compartments (Fig. 2D,E,F). We interpret these results to suggest that GRIM-19 is normally localized to mitochondria, and in IFN/RA-treated cells there could be redistribution between mitochondrial and nonmitochondrial localizations.<sup>7,8</sup> Using the fractionation method and Western blot analysis, major mitochondrial and minor nuclear localization of GRIM-19 after IFN/RA treatment in the MCF-7 breast carcinoma cell line has been documented.<sup>23</sup> We used cell fractionation and Western blotting methods to detect GRIM-19 in the cytosolic fraction for determining whether an increase in cytoplasmic GRIM-19 occurs after IFN/RA treatment. These experiments did not detect GRIM-19 in the cytosolic fraction (data not shown). Therefore, the redistribution of GRIM-19 in SH-SY5Y cells could only be addressed by immunostaining. It is likely that GRIM-19 enters other cellular compartments following IFN/RA and joins other protein complexes for driving cell death. Our recent data show that GRIM-19 can associate with a cellular protease, HtrA2, and inhibit an antiapoptotic factor, XIAP (D.V. Kalvakolanu et al., unpublished observations). Future studies are aimed at understanding these complexes.

### Increased immunoreactivity of GRIM-19 in cerebral ischemia

In cerebral permanent focal ischemia of the mouse, expression changes of 56 transcriptionally altered genes were detected by an advanced fragment display technique (restriction-mediated differential display).<sup>15</sup> Results showed that after 24 h of permanent focal ischemia, there was an increase in mRNA expression of GRIM-19 in the ischemic hemisphere compared with the nonischemic hemisphere of the brain. Previous analyses did not detect changes in GRIM-19 mRNA expression at early time points of permanent focal ischemia.<sup>15</sup> Therefore, we focused the study on 24 h after ischemia.

In the present study, we quantified and determined the cellular distribution of GRIM-19 after 24 h of permanent focal ischemia. Ischemia-induced brain damage was confirmed by staining the hemispheres with TTC staining. A massive infarct on the occluded side, including the caudoputamen and overlying cortex, was observed (Fig. 2G). Mitochondria and total RNA were isolated from the ischemic (ipsilateral) and nonischemic (contralateral) hemispheres. The mitochondria were further separated into synaptosomes and nonsynaptic fractions by Percoll-gradient centrifugation. The results are shown in Figure 3. In synaptosomes from the ipsilateral hemisphere, the GRIM-19 protein level increased by >50% compared with the contralateral hemisphere (Fig. 3A,B), whereas no changes in GRIM-19 protein levels were observed in non-synaptic mitochondria. Probing the blots with another mitochondrial protein, porin, showed no changes in its level, suggesting that the changes in GRIM-19 are specific (Fig. 3A,B). Considering that there is extensive necrosis in the affected region, the increase in GRIM-19 expression in the surviving cells would be likely to be greater. To confirm that there is an increase in GRIM-19 expression in the affected region of the brain, total RNA isolated from the contralateral and ipsilateral hemispheres was subjected to quantitative RT-PCR as

described in Materials and Methods. The results are shown in Figure 3C,D. There was a significant 32-fold increase in GRIM-19 mRNA levels in the ipsilateral hemisphere compared with the contralateral hemisphere. The changes in mRNA expression were found to be much higher than those of the protein levels. One possible explanation for the difference observed between mRNA and protein levels could be that focal ischemia induces inhibition of protein synthesis.<sup>24</sup> Thus, our results confirm and extend the observation that GRIM-19 is upregulated in the affected brain region after focal ischemia.

Isolated brain mitochondria originate from many cell types, including neurons, astrocytes, and oligodendrocytes. The greater ratio of GRIM-19/porin in synaptosomal fractions of the ipsilateral hemisphere compared with the contralateral one suggests that changes in expression of GRIM-19 after ischemia most likely occur in neurons than in astrocytes because the synaptosomal fraction is more enriched with neuronal mitochondria. To confirm this, we compared the expression of GRIM-19 in mitochondria from primary cultures of cortical neurons and astrocytes. Mitochondria from cultured primary cells (cortical neurons and astrocytes) were isolated by the nitrogen cavitation technique, which allows for isolation of functionally and morphologically intact mitochondria. The ratio of GRIM-19/porin was significantly greater in neuronal mitochondria than in astrocytic mitochondria (Fig. 4A). These data suggest that there is a heterogeneous distribution of GRIM-19 between neurons and astrocytes and that GRIM-19 expression is elevated after ischemia primarily in neuronal (synaptic) mitochondria.

### **GRIM-19, oxidative stress, protein carbonylation, and ischemic damage**

GRIM-19 is a subunit of complex I of the OXPHOS of mitochondria. Complex I consist of 46 proteins, catalyzes the first step of the electron transfer chain reaction, and is one of the major sites of ROS generation<sup>4</sup> and also a target of oxidative stress. To correlate changes in GRIM-19 protein with the extent of oxidative stress, we measured oxidative modification of proteins by Oxyblot in the same samples that showed changes in GRIM-19 protein levels. The results are shown in Figure 4B.

Oxidative modification of proteins by oxygen free radicals leads to the introduction of carbonyl groups into protein sidechains by a site-specific mechanism and is a sensitive measure of oxidative injury.<sup>25</sup> Detection of these groups can be achieved by derivatization in reaction with dinitrophenylhydrazine (DNPH). Lysates from synaptosomal fractions of rat brain were treated with DNPH, resolved on the gel, and subjected to Western blot analysis with primary antibody specific to the DNP moiety of the proteins. Oxidative modification of proteins in Oxyblot in the synaptosomal fractions of rat brain subjected to focal ischemia demonstrated a higher oxidative state; thus, oxidative injury in the ipsilateral hemisphere is documented in the infarct area.

In a genetic screen that was designed to define the critical factors involved in IFN/RA-induced apoptosis, we identified GRIM-19 as a novel cell death regulator protein.<sup>7</sup> Subsequently, it was discovered that GRIM-19 is part of respiratory chain complex, as a subunit of complex I. This predicted a mitochondrial localization of GRIM-19. To confirm this, we determined the localization of GRIM-19 in a human neuroblastoma cell line, SH-SY5Y, that was transfected with mitochondrially targeted eYFP. The results showed colocalization of GRIM-19 with eYFP in SH-SY5Y cells. Thus, our results confirm the predominant localization of GRIM-19 to mitochondria.

Mitochondria have long been considered as mediators of cell death in acute brain ischemic injury. Both oxidative stress and apoptotic pathways have been implicated in the neuronal death after focal ischemia. The levels of GRIM-19 protein are increased in synaptic mitochondria of the affected ipsilateral hemisphere compared with the contralateral hemisphere. Neuronal

mitochondria have higher levels of GRIM-19 than mitochondria from astrocytes. In addition, increased GRIM-19 protein levels in the ipsilateral hemisphere are found to correlate with increased oxidative stress. Consistent with our observation, a recent study by Huang et al.<sup>26</sup> showed that exposure of cultured cells to IFN/RA induces GRIM-19, increases ROS, induces apoptosis and knockdown of GRIM-19, decreases ROS, and protects against apoptosis.<sup>26</sup> In summary, the results presented in this study suggest a possible role for GRIM-19 in neuronal cell death in focal ischemia, possibly via oxidative stress.

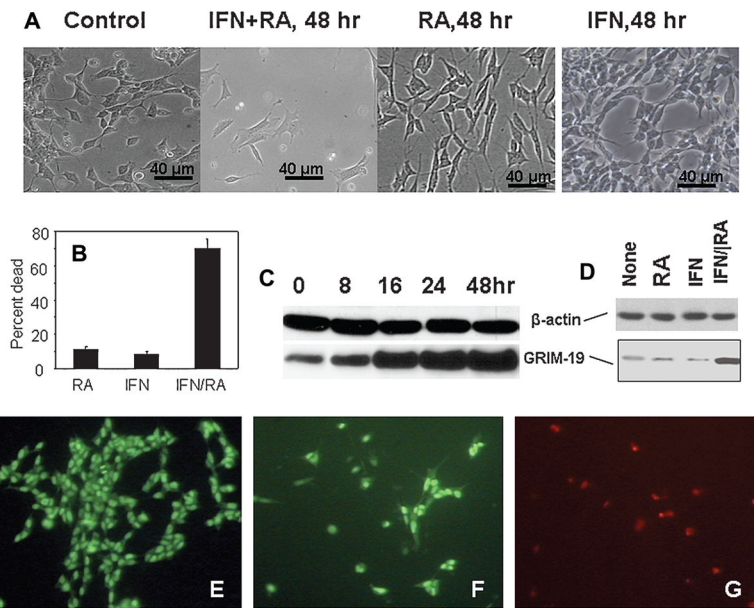
## Acknowledgements

We thank Ms. Irene Hopkins and Ms. L. Rahman for technical assistance. This work was supported by NIH NS34152 (G.F.), U.S. Army DAMD17-99-1-9483 (G.F.), CA 105005 (D.V.K.), and CA78282 (D.V.K.).

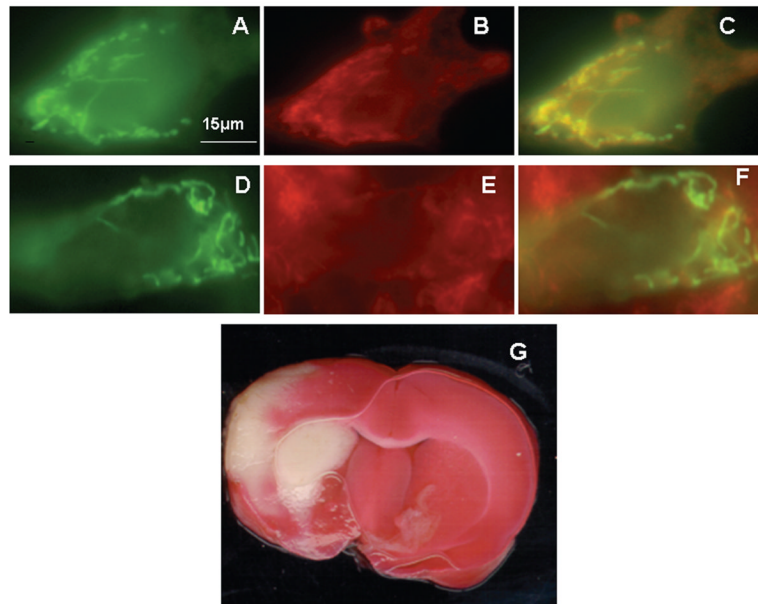
## References

1. Starkov AA, Chinopoulos C, Fiskum G. Mitochondrial calcium and oxidative stress as mediators of ischemic brain injury. *Cell Calcium* 2004;36:257–264. [PubMed: 15261481]
2. Polster BM, Fiskum G. Mitochondrial mechanisms of neural cell apoptosis. *J Neurochem* 2004;90:1281–1289. [PubMed: 15341512]
3. Mehrabian Z, Liu LI, Fiskum G, Rapoport SI, Chandrasekaran K. Regulation of mitochondrial gene expression by energy demand in neural cells. *J Neurochem* 2005;93:850–860. [PubMed: 15857388]
4. Andreyev AY, Kushnareva YE, Starkov AA. Mitochondrial metabolism of reactive oxygen species. *Biochemistry (Mosc)* 2005;70:200–214. [PubMed: 15807660]
5. Moore DM, Kalvakolanu DV, Lippman SM, Kavanagh JJ, Hong WK, Borden EC, Paredes-Espinoza M, Krakoff IH. Retinoic acid and interferon in human cancer: mechanistic and clinical studies. *Semin Hematol* 1994;31(Suppl 5):31–37. [PubMed: 7831583]
6. Lindner DJ, Kolla V, Kalvakolanu DV, Borden EC. Tamoxifen enhances interferon-regulated gene expression in breast cancer cells. *Mol Cell Biochem* 1997;167:169–177. [PubMed: 9059994]
7. Angell JE, Lindner DJ, Shapiro PS, Hofmann ER, Kalvakolanu DV. Identification of GRIM-19, a novel cell death-regulatory gene induced by the interferon-beta and retinoic acid combination, using a genetic approach. *J Biol Chem* 2000;275:33416–33426. [PubMed: 10924506]
8. Zhang J, Yang J, Roy SK, Tininini S, Hu J, Bromberg JF, Poli V, Stark GR, Kalvakolanu DV. The cell death regulator GRIM-19 is an inhibitor of signal transducer and activator of transcription 3. *Proc Natl Acad Sci USA* 2003;100:9342–9347. [PubMed: 12867595]
9. Seo T, Lee D, Shim YS, Angell JE, Chidambaram NV, Kalvakolanu DV, Choe J. Viral interferon regulatory factor 1 of Kaposi's sarcoma-associated herpesvirus interacts with a cell death regulator, GRIM19, and inhibits interferon/retinoic acid-induced cell death. *J Virol* 2002;76:8797–8807. [PubMed: 12163600]
10. Maximo V, Botelho T, Capela J, Soares P, Lima J, Taveira A, Amaro T, Barbosa AP, Preto A, Harach HR, Williams D, Sobrinho-Simoes M. Somatic and germline mutation in GRIM-19, a dual function gene involved in mitochondrial metabolism and cell death, is linked to mitochondrion-rich (Hurthle cell) tumours of the thyroid. *Br J Cancer* 2005;92:1892–1898. [PubMed: 15841082]
11. Fusco A, Viglietto G, Santoro M. Point mutation in GRIM-19: a new genetic lesion in Hurthle cell thyroid carcinomas. *Br J Cancer* 2005;92:1817–1818. [PubMed: 15900303]
12. Fearnley IM, Carroll J, Shannon RJ, Runswick MJ, Walker JE, Hirst J. GRIM-19, a cell death regulatory gene product, is a subunit of bovine mitochondrial NADH:ubiquinone oxidoreductase (complex I). *J Biol Chem* 2001;276:38345–38348. [PubMed: 11522775]
13. Huang G, Lu H, Hao A, Ng DC, Ponniah S, Guo K, Lufei C, Zeng Q, Cao X. GRIM-19, a cell death regulatory protein, is essential for assembly and function of mitochondrial complex I. *Mol Cell Biol* 2004;24:8447–8456. [PubMed: 15367666]
14. Kalvakolanu DV. The GRIMs: a new interface between cell death regulation and interferon/retinoid induced growth suppression. *Cytokine Growth Factor Rev* 2004;15:169–194.
15. Schneider A, Laage R, von Ahsen O, Fischer A, Rossner M, Scheek S, Grunewald S, Kuner R, Weber D, Kruger C, Klaussner B, Gotz B, Hiemisch H, Newrzella D, Martin-Villalba A, Bach A,

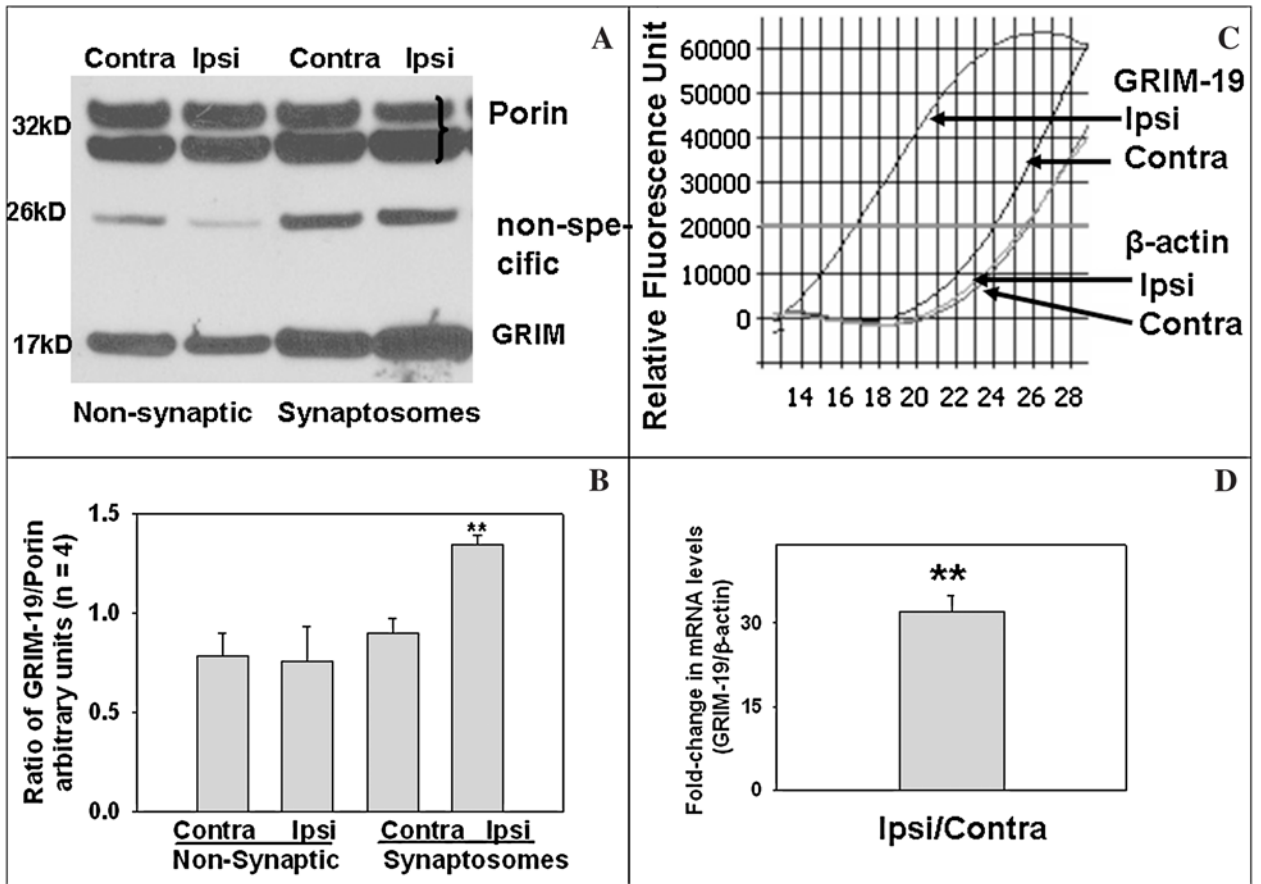
- Schwaninger M. Identification of regulated genes during permanent focal cerebral ischemia: characterization of the protein kinase 9b5/MARKL1/MARK4. *J Neurochem* 2004;88:1114–1126. [PubMed: 15009667]
16. Yavin Z, Yavin E. Survival and maturation of cerebral neurons on poly(L-lysine) surfaces in the absence of serum. *Dev Biol* 1980;75:454–459. [PubMed: 6989691]
  17. Booher J, Sensenbrenner M. Growth and cultivation of dissociated neurons and glial cells from embryonic chick, rat and human brain in flask cultures. *Neurobiology* 1972;2:97–105. [PubMed: 4572654]
  18. Bederson JB, Pitts LH, Tsuji M, Nishimura MC, Davis RL, Bartkowski H. Rat middle cerebral artery occlusion: evaluation of the model and development of a neurologic examination. *Stroke* 1986;17:472–476. [PubMed: 3715945]
  19. Kristian T, Weatherby TM, Bates TE, Fiskum G. Heterogeneity of the calcium-induced permeability transition in isolated non-synaptic brain mitochondria. *J Neurochem* 2002;83:1297–1308. [PubMed: 12472884]
  20. Lowry OH, Rosebrough NJ, Farr AL, Randall RJ. Protein measurement with the Folin phenol reagent. *J Biol Chem* 1951;193:265–275. [PubMed: 14907713]
  21. Kristian T, Hopkins IB, McKenna MC, Fiskum G. Isolation of mitochondria with high respiratory control from primary cultures of neurons and astrocytes using nitrogen cavitation. *J Neurosci Methods* 2006;152:136–143. [PubMed: 16253339]
  22. Darzynikiewicz, Z.; Li, X.; Gong, J.; Hara, S.; Traganos, F. Analysis of cell death by flow cytometry. In: Studzinski, GP., editor. *Cell Growth and Apoptosis*. Newark, NJ: IRL Press; 1995. p. 143-167.
  23. Lufe C, Ma J, Huang G, Zhang T, Novotny-Diermayr V, Ong CT, Cao X. GRIM-19, a death-regulatory gene product, suppresses Stat3 activity via functional interaction. *EMBO J* 2003;22:1325–1335. [PubMed: 12628925]
  24. DeGracia DJ. Acute and persistent protein synthesis inhibition following cerebral reperfusion. *J Neurosci Res* 2004;77:771–776. [PubMed: 15334596]
  25. Lenz AG, Costabel U, Shaltiel S, Levine RL. Determination of carbonyl groups in oxidatively modified proteins by reduction with tritiated sodium borohydride. *Anal Biochem* 1989;177:419–425. [PubMed: 2567130]
  26. Huang G, Chen Y, Lu H, Cao X. Coupling mitochondrial respiratory chain to cell death: an essential role of mitochondrial complex I in the interferon-beta and retinoic acid-induced cancer cell death. *Cell Death Differ* 2006;14:327–337. [PubMed: 16826196]

**FIG. 1.**

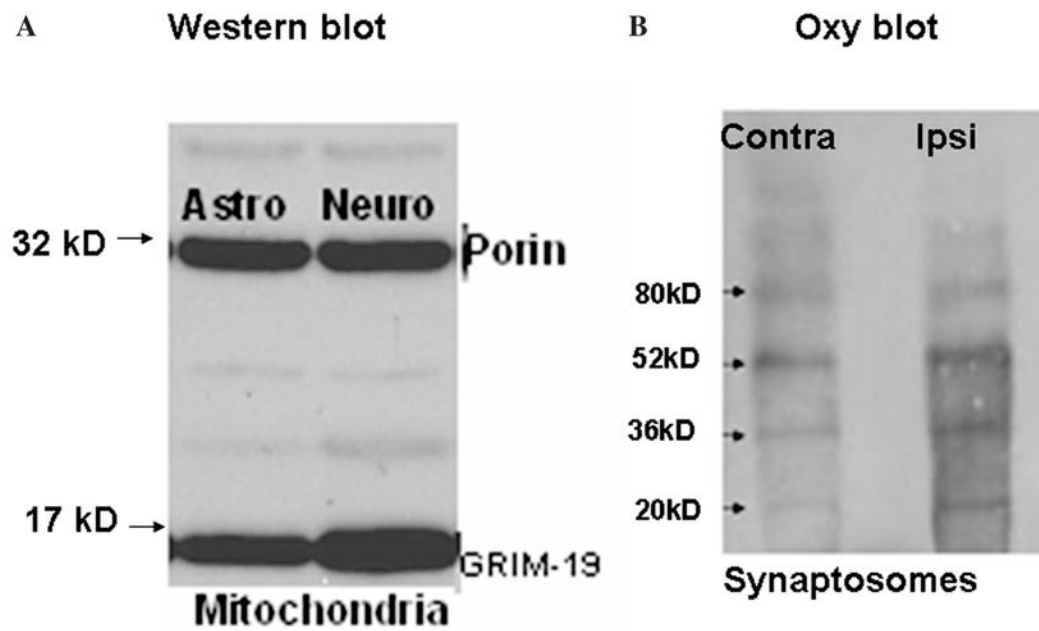
Effect of exposure to IFN/RA on cell death and GRIM-19 protein levels in SH-SY5Y human neuroblastoma cells. Human neuroblastoma cell line SH-SY5Y cells were exposed to IFN and RA for various periods of time. **(A)** Phase-contrast microscopy showing the morphology and extent of cell death at 48 h. Control: vehicle alone; cells were treated with IFN, RA, and IFN/RA for 48 h. **(B)** Flow cytometric analysis of cell death. Cells were exposed to various agents for 48 h and stained with PI and subjected to flow cytometry. The percentage of dead cells (sub-G1 peak) was determined, and values from triplicate samples were plotted. **(C and D)** Western blot analyses for GRIM-19 expression. Total protein from cell extracts prepared at various times after exposure to IFN/RA was separated by SDS-PAGE, transferred to PVDF membrane, and probed either with  $\beta$ -actin antibody or with anti-GRIM-19 antibody, as described in Materials and Methods. A 15-fold increase in GRIM-19 protein levels compared with  $\beta$ -actin was seen at 48 h. **(E, F, and G)** SH-SY5Y neuroblastoma cells seeded at a low density were treated for 48 h with either vehicle **(E)** or IFN/RA **(F and G)** and then stained with SYTO-13 **(E and F)** or with PI **(G)**.



**FIG. 2.** Localization of GRIM-19 in neuronal cells and effect of permanent focal ischemia-induced infarction in rat brain. SH-SY5Y cells were transfected with a mito-eYFP vector. The transfected cells were fixed and then immunolabeled with anti-GRIM antibody. **(A)** eYFP fluorescence (green). **(B)** Anti-GRIM-19 antibody (Alexa Fluor 546, red fluorescence). **(C)** Merged image of **A** and **B**. Mito-eYFP-transfected cells were treated with IFN/RA for 16 h, fixed, and then immunolabeled with anti-GRIM antibody. **(D)** eYFP fluorescence (green). **(E)** anti-GRIM-19 antibody (Alexa Fluor 546, red fluorescence). **(F)** Merged image of **D** and **E**. Note colocalization of green and red fluorescence to mitochondria in **C**. **(G)** TTC staining of coronal section of rat brains subjected to 24 h permanent focal ischemia, showing a massive infarct on the occluded side, including the caudoputamen and overlying cortex.

**FIG. 3.**

Quantification of changes in GRIM-19 in ipsilateral and contralateral hemispheres in neurons and astrocytes and effect of ischemia on oxidative modification of proteins. (A) Nonsynaptic and synaptic mitochondria were prepared from contralateral and ipsilateral hemispheres. Proteins were separated by SDS-PAGE, subjected to Western blot transfer, and probed with GRIM-19 or with another mitochondrial protein, porin. (B) The intensities of the bands were quantified, and percent changes were calculated. Intensity/area ratio for GRIM-19 band/porin band were mito-contralateral, 0.8; mito-ipsilateral, 0.78; synaptosomes contralateral, 0.83; synaptosomes ipsilateral, 1.25, which shows a 51% increase. (C) Total RNA isolated from contralateral and ipsilateral hemispheres was subjected to QRT-PCR with GRIM-19 or  $\beta$ -actin primers. The  $\Delta$ Ct cycles are shown. (D) The fold changes were calculated. A significant increase in GRIM-19 mRNA levels was observed in the ipsilateral compared with the contralateral hemispheres after ischemia.

**FIG. 4.**

(A) Mitochondria were isolated from primary rat cortical neurons and astrocytes, separated by SDS-PAGE, subjected to Western blot transfer, and probed with GRIM-19 or with another mitochondrial protein, porin. (B) Oxyblot detection of synaptosomal proteins from ipsilateral and contralateral hemispheres shows a higher oxidative state; thus, oxidative injury is higher in the ipsilateral hemisphere.